Sensors & Actuators: A. Physical 387 (2025) 116401

Contents lists available at ScienceDirect

Sensors and Actuators: A. Physical

journal homepage: www.journals.elsevier.com/sensors-and-actuators-a-physical

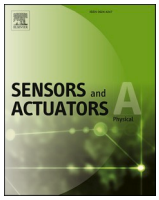

Viscosity measurement of small volume liquid samples in a falling body viscometer employing compact electromagnetic actuation and sensing

Xinjing Huang [a], Hongbin Zhang [a], Xu Bian [a,b], Kun Zhang [c], Jian Li [a], Jinyu Ma [a,*]

[a] State Key Lab Precision Measurement Technology and Instruments, Tianjin University, Tianjin 300072, China
[b] Tianjin Renai College, Tianjin 300072, China
[c] Shandong Non-Metallic Materials Institute, Jinan 250031, China

ARTICLE INFO

Keywords:
Falling body method
Liquid viscosity
Electromagnetic principle
Viscosity measurement

ABSTRACT

Falling body (FB) methods have unique advantages in the viscosity measurement of high-temperature and high-pressure liquids because of the durability of the sensing parts and their suitability for carrying out measurements in a metal closed cylindrical chamber (CCC). However, the current methods usually use two coils fixed away from each other to sense the position and speed of the FB, which leads to a long travel distance of the FB, a large CCC, and the inability of the FB to automatically reset. This paper proposes a novel compact liquid viscosity measurement device using only one coil outside a stainless steel CCC to sense the moving speed of the iron FB and uses another coil fixed close to the sensing coil to reset the FB. Both the FB travel distance and the CCC size are very small. The stable velocity of the FB is directly measured according to the linear relationship between the impedance of the sensing coil and the position of the FB, and then the velocity is used to calculate the liquid viscosity. Viscosity tests were conducted on four standard viscosity liquids at different temperatures. The results show that for liquids with a viscosity range of 4.417 mPa·s~88.44 mPa·s, the descent time of FBs is between 2 and 19 s. The relative error is concentrated within 5 %, and the standard deviation falls between 0.01 mPa·s and 1.46 mPa·s. Within the 95 % confidence interval ($k = 2$), the expanded uncertainty of the four liquids viscosity measurement at different temperatures ranges from 0.74 mPa·s to 2.93 mPa·s, and the relative expanded uncertainty ranges from 6.32 % to 10.6 %. The measurement results have high accuracy and repeatability.

1. Introduction

Viscosity is an intrinsic physical property of a fluid that reflects the internal friction between molecules when the fluid is subjected to external forces [1]. The measurement of liquid viscosity can be used to evaluate the flow characteristics of a liquid, which is important for ensuring production efficiency and safety in fields such as oil and gas development [2], coal liquefaction [3,4], the chemical industry, and power equipment operation. In these fields, it is often necessary to measure the viscosity of high-temperature and high-pressure liquids. Owing to the limited high-temperature and high-pressure environment, the measurement of liquid viscosity needs to be carried out in a closed chamber, using high-temperature and high-pressure resistant materials to contact the liquid, or using a non-contact sensor to obtain the viscosity information.

Commonly used methods for measuring the viscosity of high-temperature and high-pressure liquids include the capillary method, rotation method, falling body (FB) method, and vibration method.

Capillary viscometers have long been used with highly viscous liquids and have a high level of accuracy. The widely used Cannon standards, for example, have their viscosities determined in this way. Rotational viscometers are very convenient for routine measurements. However, when measuring the viscosity of high-temperature and high-pressure liquids, the rotational viscometer has a complex structure and requires many parts [5,6]. Vibrating wire viscometer has a wide viscosity measurement range. But the vibrating wire viscometer requires a longer container to increase the length of the metal wire and make it easier to vibrate, so the measurement device is relatively large [7,8].

Compared with the capillary method, rotary method, and vibration method, the FB method has the unique advantages of a simple structure and ease of use of a closed cylindrical chamber (CCC) for viscosity measurement, especially when measuring the viscosity of small volume liquids under high temperature and high pressure conditions. The measurement principle allows the FB to fall freely in the measured liquid

* Corresponding author.
E-mail address: jinyu.ma@tju.edu.cn (J. Ma).

https://doi.org/10.1016/j.sna.2025.116401
Received 5 November 2024; Received in revised form 8 February 2025; Accepted 25 February 2025
Available online 26 February 2025

in a CCC, and the FB is subject to its own gravity, the upward viscous force provided by the liquid, and buoyancy. Because the magnitude of the viscous force is positively related to the velocity of the FB, when the FB is balanced by the three forces, it can reach a constant speed, and then the viscosity value can be calculated by measuring the time difference between the two fixed points in the vertical channel. The development of the FB viscometer can be traced back to Bridgman [9,10] who used a falling cylinder to test the viscosity of 43 different fluids under high pressure, and Bridgman pointed out that the viscosity of the fluid is positively related to the falling time of the falling cylinder. The theory of measuring liquid viscosity using the FB method has been continuously improved. However, when the FB method is applied to measure the viscosity of liquids in high-temperature and high-pressure CCCs, two major problems need to be solved: how to detect the position of the FB in the CCC without contact and how to control the FB to return to the initial position without contact to carry out the next measurement.

To detect the position of the FB, the mainstream method is to form a Wheatstone bridge with two inductance coils wound around the CCC. When the FB passes through the two coils in sequence, it causes an imbalance in the electrical signal of the bridge, which is amplified, shaped and used to trigger the timer on and off. By measuring the time it takes for the FB to pass through the two coils, the viscosity of the liquid can be calculated. Harris [11] proposed a high-pressure FB viscometer on the basis of this method. To accurately distinguish the imbalance signal when the FB passes the two coils in sequence, the FB must not affect the inductance change of the two coils simultaneously during the falling process. Therefore, the distance between the two coils is greater than 100 mm, the CCC and the measurement cycle are both very long, and more liquid samples are required to fill the CCC. Bair [12] proposed a compact FB viscometer that uses a variable differential transformer to measure the fall time of the FB. For falling times greater than about 100 s, accuracy is reduced due to instrumentation drift. Tanaka [13,14] used a Pyrex glass tube as a CCC, and measured the position of the FB through a laser beam and a phototransistor. Jackson [15,16] used a high-pressure glass window to seal the container tube, and used laser Doppler technology to measure the falling speed of the FB instead of measuring the time. However, this optical method has limitations when sealing, so they are difficult to extend to high-pressure environments.

At present, there is still no method suitable for automatic reset of the FB in the miniaturized falling body viscometer. Wang [17] developed a set of high-pressure liquid viscosity measurement systems based on the principle of the FB method, which can measure viscosity in the temperature range of 293–363 K and the pressure range of 0.1–45 MPa. However, the FB reset method was not used in this study, and only a single measurement could be carried out. Schaschke et al. [18,19] comprehensively evaluated the performance of an FB viscometer by combining experimental data and fluid dynamics calculation results. However, the reset of the FB requires the entire pressure vessel to be rotated 180°, resulting in a very complicated operation process and a long measurement period, which takes 398–2800 s. In the FB high-pressure viscometer proposed by Harris [11], the reset of the FB also requires the pressure vessel to rotate 180°. This reset method requires much space, and the measurement time is long, ranging from 20 s to 10,000 s. Owing to the long movement range of the FB, it is impossible to reset the FB through the electromagnetic force generated by a single coil. Irving and Barlow [20] developed an automated high-pressure liquid viscometer, which realizes not only the movement and positioning of the FB through the alternating energization of a series of coils but also the automation of viscosity measurement. However, the use of multiple coils to reset the FB results in a very complex structure and large volume of the entire instrument. Sagdeev et al. [21,22] designed and manufactured a liquid viscometer on the basis of the principle of the FB method with an automatic resetting device with a traction solenoid placed outside the CCC moving up to drive FB resetting. Owing to the large moving distance of the FB while passing through two detection coils, a strong electromagnetic force is needed to ensure the reset of the FB, resulting in a larger traction solenoid. Solving the problem of FB position detection and reset while ensuring the miniaturization and simple structure of the device is important for the development of FB viscometers.

The traditional FB methods use double coils to measure the falling time of the FB and then calculate the FB speed and liquid viscosity. Since the two coils are far apart, the FB travels a long distance. This leads to difficulty in resetting the FB, the large volume of the measuring device, the long measurement time, and the large amount of liquid sample needed.

This paper uses the linear relationship between the impedance of a single coil and the position of the FB to measure the speed of the FB to ensure that the distance of travel of the FB is very short. This greatly reduces the length of the measurement chamber, thereby enabling the use of a fixed-position, low-power coil to reset the FB. This method can make the liquid viscosity measurement device more compact, decrease the measurement time, and require less sample.

In this work, a novel compact device for measuring liquid viscosity in a CCC with a simple structure, small size, small sample quantity and fast detection speed is designed. This device uses only one coil outside a stainless steel CCC to sense the moving speed of the iron FB and uses another coil fixed close to the sensing coil to reset the FB. Both the FB travel distance and the CCC size are very small. By finite element simulation, the falling rules of FBs of different sizes in liquids with different viscosities and the relationship between the FB position and coil impedance are investigated. Falling bodies of different sizes are designed according to the division of the measurement range. A method is designed to calculate the liquid viscosity by measuring the change rate of the coil impedance. By measuring the viscosity of four reference liquids—squalane, diisodecyl phthalate, the standard material GBW(E) 130720, and the standard material GBW(E)130615—at different temperatures and comparing them with literature and standard material property values, the feasibility of the measuring device and the correctness and repeatability of the measurement results are verified. According to the practical application requirements, the technical advantages of the scheme are analyzed, and future development directions are noted.

2. Measurement methods

2.1. Measurement principle

The principle of measuring liquid viscosity via the FB method is shown in Fig. 1. The radius of the FB is r_1, the length is h_1, and the radius of the cylinder where the FB is located is r_2. The FB coaxially falls downward at a stable speed in the cylinder under the action of gravity. There is a velocity gradient in the liquid, and the liquid in contact with

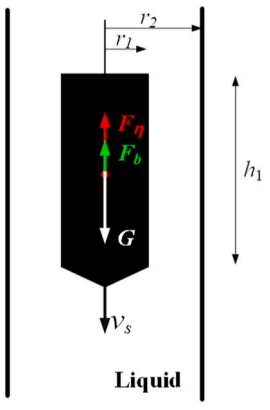

Fig. 1. Schematic of the FB method.

the tube wall is stationary. The FB is affected by gravity G, buoyancy force F_b and viscous force F_η simultaneously, among which the viscous force increases with increasing FB speed. When the three forces are balanced, the falling speed reaches a stable value v_s. The expression of the liquid viscosity η is shown in Eq. (1) [19].

$$\eta = \frac{mg}{2\pi v_s h_1}\left(1-\frac{\rho_{liq}}{\rho_s}\right)\left[\ln\frac{r_2}{r_1}-\frac{r_2^2-r_1^2}{r_2^2+r_1^2}\right] \tag{1}$$

where m is the mass of the FB, ρ_{liq} is the density of the liquid to be measured, and ρ_s is the density of the FB. Eq. (1) can be rewritten as:

$$\eta = \frac{A}{v_s}\left(1-\frac{\rho_{liq}}{\rho_s}\right) \tag{2}$$

where A is the instrument coefficient, and its value is as follows:

$$A = \frac{mg\left[\ln\frac{r_2}{r_1}-\frac{r_2^2-r_1^2}{r_2^2+r_1^2}\right]}{2\pi h_1} \tag{3}$$

Eq. (2) shows that the liquid viscosity η is inversely proportional to the stable speed v_s of the FB.

The instrument coefficient A can be obtained by calibrating the standard liquid with known viscosity, and then the liquid viscosity can be calculated by measuring the stable speed of the FB when it falls freely in different liquids.

2.2. Implementation scheme

On the basis of the above measurement principles, a device for measuring liquid viscosity in a CCC based on electromagnetic drive and sensing is designed, as shown in Fig. 2. The stainless steel tube and plug form a CCC. The inside of the CCC is filled with liquid, the iron FB moves inside the CCC, and the movement range consists of the upper and lower limits of the CCC. Two coils are wound around the outer wall of the stainless steel tube, namely, the driving coil and the sensing coil. The liquid to be measured is filled in the CCC and then a FB of the appropriate range is placed into the CCC. The driving coil generates a magnetic field after passing the current, which is used to attract the FB to move vertically upward until the FB reaches the upper limit and completes its reset. After the driving coil is powered off, the magnetic field disappears, and the FB moves vertically downward under the combined action of gravity, viscosity, and buoyancy until it reaches a stable speed. By measuring the change in the impedance value of the sensing coil, the falling process of the FB is monitored, and by measuring the change rate in the impedance value of the sensing coil, the stable speed of the FB is obtained. After the instrument coefficient is calibrated using a standard liquid with known viscosity, the liquid viscosity can be determined by the ratio of the change rate of the coil impedance during the free fall of the FB in different liquids.

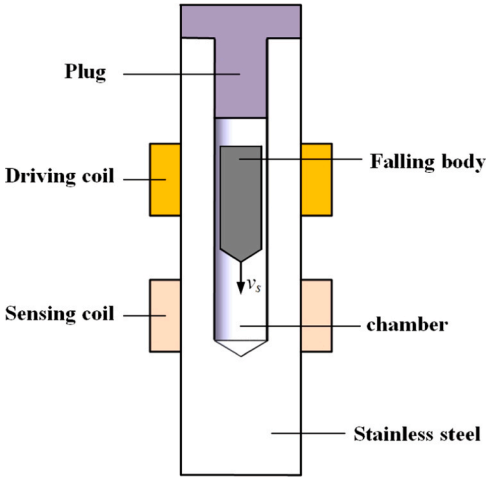

Fig. 2. Schematic of the composition of the liquid viscosity measurement device.

When the radius r_1 of the FB is close to the inner radius r_2 of the stainless steel tube, the FB quickly reaches a stable speed v_s after the moment of free fall. A reasonable design of r_1 and r_2 can make the acceleration process very short, and the falling process of the FB can be regarded as moving at a constant speed v_s. This finding is verified in Section 3, which presents the simulation verification. By using FBs with r_1 and r_2 close to each other, the FB can reach a stable speed after falling a very short distance. Thus, the beneficial effect of decreasing the movement range can be achieved. Moreover, because the movement range of the FB is short, the reset of the FB can be achieved through the electromagnetic force generated by the driving coil fixed very close to the sensing coil.

When an iron FB passes through the sensing coil, the electromagnetic impedance of the sensing coil changes, and the corresponding relationship between the position of the FB and the impedance of the sensing coil is determined. In some regions near the coil, the change in coil impedance and the position of the FB present a linear relationship. This finding is verified in Section 3, Simulation Verification. Moreover, in the linear region, when the FB moves at a constant speed v_s, the change rate of the coil impedance is proportional to the stable speed v_s of the FB. Therefore, the stable speed v_s can be characterized by measuring the change rate of the coil impedance.

3. Simulation verification

In this section, the velocity of the FB and the relationship between the position of the FB and the coil impedance are verified via finite element simulations.

3.1. Velocity of the FB

The velocity of the FB during its fall in the liquid is investigated via the finite element simulation software COMSOL. A 2D rotational axisymmetric model was constructed, as shown in Fig. 3(a). During the actual fall of the FB, the liquid underneath the FB is displaced upward, which is ensured in the finite element simulation by setting up slip conditions for the FB and the cylindrical chamber wall, where the cylindrical chamber wall moves upward and the FB remains stationary.

The inner radius of the cylindrical chamber r_2 is 4 mm, the length is 60 mm, the radius of the FB r_1 is 3.5 mm (the parameter to be swept), and the height h_1 is 20 mm. The material of the FB is pure iron, and the density is set 7800 kg/m^3 . The laminar flow is selected as the physical field of the simulation, the lower boundary of the model is set as the inlet of the fluid, the upper boundary of the model is set as the outlet of the fluid, the density of the fluid is 1000 kg/m^3, and the viscosity η is set as the parameter to be swept. The relative initial velocity of the fluid and the FB is 0. The symmetric condition is set, assuming that the fluid motion is axisymmetric about the axis of rotation. The boundary condition is set to “no-slip” for the boundary of the FB and “slip” for the inner cylindrical wall of the chamber. The mesh is set as a physical field-controlled mesh, the mesh element size is selected as Ultrafine, and the domain is meshed as shown in Fig. 3(b). The radius of the FB r_1 is swept parametrically, the transient study is added to simulate the first 0.1 s of the relative motion between the FB and the liquid, and the simulation step size is 0.002 s.

The first 0.1 s of the fall process of the FB is simulated in a liquid with a viscosity of 11 mPa·s, and the simulation step size is 0.001 s. The simulation results of the variation in the falling velocity with time of the FBs of different radii in the liquid are shown in Fig. 3(c). The FB in the liquid experiences accelerated falling and maintains uniform motion after reaching a stable velocity. Different radii of the FB in the same

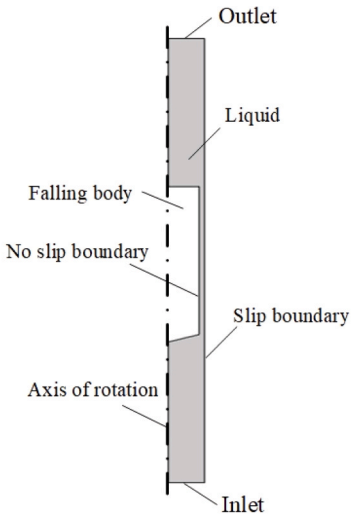

(a) Simulation model

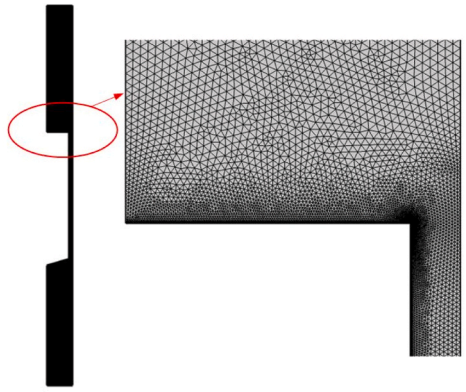

(b) Mesh

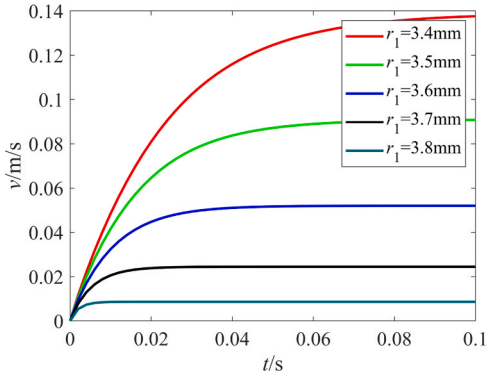

(c) Simulation results

Fig. 3. Velocities of the falling bodies with different r_1 values.

liquid have different stable velocities and different acceleration times. The closer the radius of the FB is to the inner radius of the cylindrical chamber, the shorter the acceleration times and the lower the steady-state speed.

The radius of the FB r_1 was 3.8 mm, and the liquid viscosity η was parametrically swept. η was 11 mPa·s, 21 mPa·s, 31 mPa·s, 41 mPa·s, 51 mPa·s, 61 mPa·s, 71 mPa·s, 81 mPa·s, and 91 mPa·s. The simulation is carried out for the first 0.02 s of the relative motion between the FB and the liquid, and the simulation step size is 0.001 s. The results of the simulation are shown in Fig. 4.

Fig. 4 shows that the greater the viscosity of the liquid is, the shorter

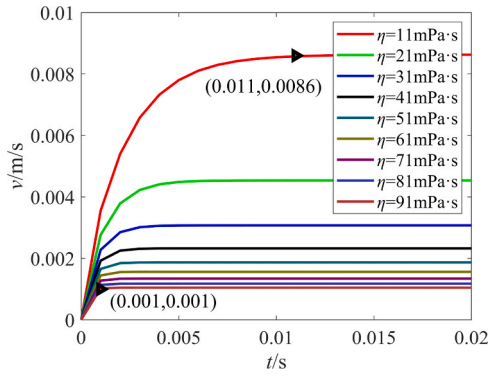

Fig. 4. Velocities of the FB within liquids of different viscosities.

the time required for the FB to reach the stabilizing velocity, and the smaller the stabilizing velocity. For example, for an FB with radius r_1 of 3.8 mm in a liquid with viscosity η of 91 mPa·s, the acceleration process takes only 1 ms, and the stabilized velocity is 0.001 m/s. If the FB falls 10 mm with the stabilized velocity, then it takes 10 s for the whole falling process. The 1 ms acceleration process accounts for only 0.01 % of the total falling time. In a liquid with a viscosity of 11 mPa·s, the acceleration phase takes only 11 ms, and the stabilized velocity is 0.0086 m/s. If the FB travels 10 mm at a steady velocity, it takes 1.163 s to fall. The 11 ms acceleration phase accounts for only 0.94 % of the total fall time.

According to the above two sets of simulation results, when the radius of FB r_1 is close to the radius of cylindrical tube r_2, the FB rapidly reaches the steady velocity v_s after the instant of free fall. The FB process can be regarded as a uniform motion with a stabilized velocity.

3.2. *Relation between the position of the FB and the impedance of the sensing coil*

The relationship between the FB position and the coil impedance is analyzed via the finite element simulation software COMSOL. A 2D rotational axisymmetric model was constructed, as shown in Fig. 5(a). The inner wall r_2, thickness, and length of the stainless steel chamber are 4 mm, 5 mm, and 100 mm, respectively. The radius r_1 and height h_1 of the FB are 3.5 mm and 20 mm, respectively. The width of the coil WH is 10 mm, and the thickness of the coil is calculated by the width of the coil WH, the number of turns of the coil N, and the diameter of the coil wire d. The FB material is pure iron, the relative permeability is 300, and the conductivity is 1.12×10^7 S/m. The relative permeability of the stainless steel is 1.2, and the conductivity is 4.03×10^6 S/m. The material of the coil is copper, the relative permeability is 1, and the conductivity is 5.99×10^7 S/m. The physical field selects the magnetic field. The coil model is set to "uniform multiple turns" with $N = 600$ and $d = 0.25$ mm. The mesh is set to "physical field control mesh", and the mesh size is selected to be "ultrafine". A frequency domain study is added to the physics, and the frequency is 500 Hz. The parametric sweeping of the FB position S is carried out, and the coil impedance value Z, resistance value R, and reactance value X are obtained with different S values. The simulation results are shown in Fig. 5(b).

In Fig. 5(b), the abscissa is the distance S in the vertical direction between the center of the FB and the center of the coil, the vertical ordinate of Fig. 5(b) is the impedance. The amount of change in reactance ΔX is defined as shown in Fig. 5(b). The definitions of the amount of change in resistance and impedance are similar. Among the impedance Z, resistance R, and reactance X, the amount of change in impedance Z is the largest. Therefore, the Z-S curve was chosen for subsequent analysis. There are two regions in the Z–S curve, where the changes in the coil impedance Z vs the relative position S are approximately linear, which is referred to as the linear region. During the design process, we used the linear zone on the right. In the linear region, the steady velocity

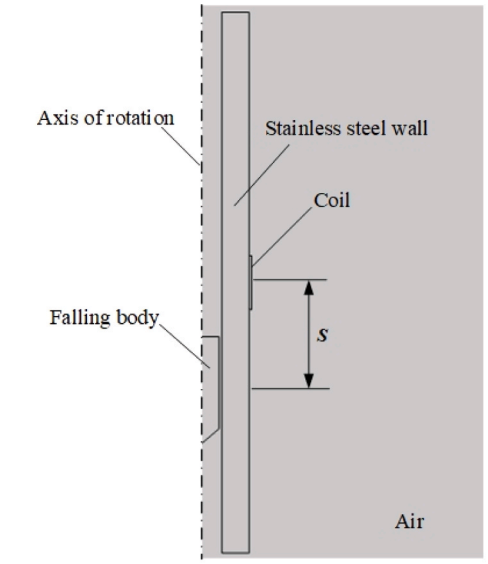

(a) Model diagram

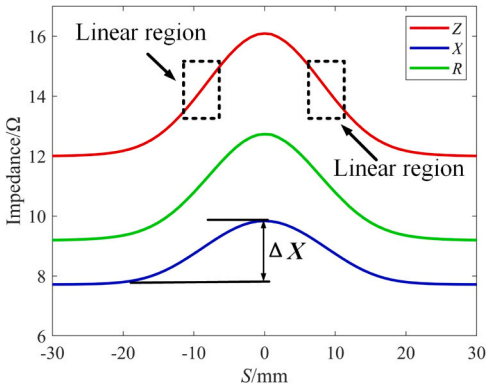

(b) Impedance change

Fig. 5. Relationships between the coil impedance and the position of the FB.

v_s of the FB can be characterized by the change rate of the coil impedance in the linear region, and then the liquid viscosity can be calculated.

Since the stable velocity v_s of the FB in the linear region is proportional to the change rate of impedance v_x,v_s=$k_x v_x$, the measurement formula is modified to Eq. 4.

$$\eta = \frac{B}{v_x}\left(1 - \frac{\rho_{liq}}{\rho_s}\right) \tag{4}$$

In Eq. 4, B=$A \cdot k_x$, since no literature has been found that provides expressions for the coil impedance when the FB is at different positions, the instrument coefficient B is obtained through calibration.

4. Experiment

4.1. Experimental apparatus

(1) CCC device for measuring liquid viscosity

The inner radius r_2 of the CCC of the stainless steel tube is 4 mm, and the wall thickness of the cylinder is 5 mm. Considering the amplitude of the impedance value Z, the length of the linear region, and the heat dissipation of the coil, the coil is designed to have $N = 1000$ turns, a width WH= 16 mm, and a wire diameter d= 0.25 mm. A cross-sectional view of the measuring device is shown in Fig. 6(a). The chamber device contains a driving coil, a sensing coil, an iron plug, an FB and a PT100.

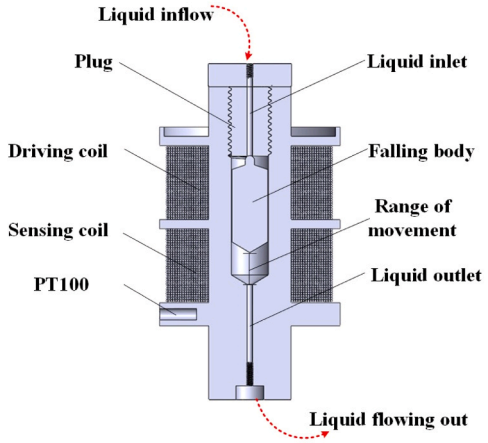

(a) Cross-sectional schematic of the chamber device

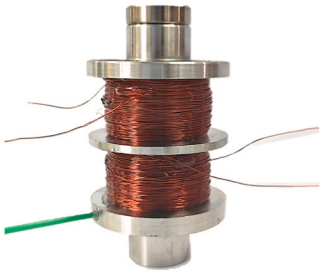

(b) Photo of the chamber device

Fig. 6. Viscosity measurement apparatus.

The driving coil is used to drive the FB to reset, and the sensing coil is used to detect the position and speed of the FB. The plug is used to limit the upward moving range of the FB and seal the chamber. A PT100 was used to detect the liquid temperature. To avoid frequent dismantling of the device for pressurization and pressure relief to change the liquid when different liquid viscosities are measured under high-temperature and high-pressure conditions, we designed liquid inlet and outlet ports for the experimental chamber device. A physical diagram of the device is shown in Fig. 6(b). The external dimensions of the device are 73 mm*39 mm.

(2) FB

The drop height h_1 is designed to be 20 mm. To accommodate liquids with different viscosities, the radius of the FB r_1 is designed according to different viscosity measurement ranges. The range of movement of the FB is 11 mm, and when the FB reaches the lower limit, Z is still in the linear region of the change in the impedance value of the sensing coil. Since the FB movement range is only 11 mm, both the measurement time and the CCC are reduced, and only 1 mL of liquid is needed to completely fill the CCC. The device is compact and simple in structure.

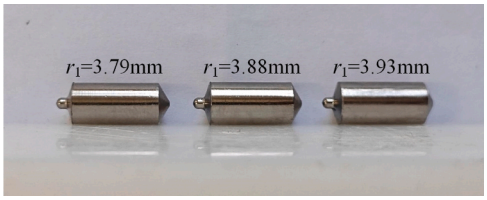

Fig. 7. Photo of the falling bodies.

The physical diagram of the FB is shown in Fig. 7. The FB is composed of pure iron material. The top of the FB is designed as an arc surface to prevent the top of the FB from freely falling due to a large viscous force after resetting. The bottom of the FB is designed as a conical surface, which is matched with the bottom of the stainless steel chamber to ensure that the movement of the FB in the chamber is coaxial during each measurement. The actual size of the FB is as follows: for liquids with viscosities ranging from 1–20 mPa·s, the radius of the FB r_1 is 3.93 mm; for liquids with viscosities ranging from 20–50 mPa·s, the radius of the FB r_1 is 3.88 mm; for liquids with viscosities ranging from 50–100 mPa·s, the radius of the FB r_1 is 3.79 mm. For the measurement of the viscosity of low-viscosity liquids, a FB with a larger radius is used to reduce the falling speed to prevent turbulence caused by the high falling speed of the FB. For high-viscosity liquids, a FB with a smaller radius is used to increase the falling speed of the FB and shorten the measurement time.

(3) Viscosity measurement system

A block diagram of the viscosity measurement system is shown in Fig. 8(a). The driving coil generates an electromagnetic force when current passes through it, and the iron plug forms an electromagnet in the magnetic field, which is used to increase the attraction force on the FB. The impedance detection circuit is employed to monitor the impedance Z of the sensing coil, which is used to ascertain the position of the FB and to estimate its falling speed. The impedance data at different moments are transmitted to the host computer by the microcontroller for further analysis and calculation. The temperature of the liquid was measured by a PT100. A photo of the measurement system is shown in Fig. 8(b).

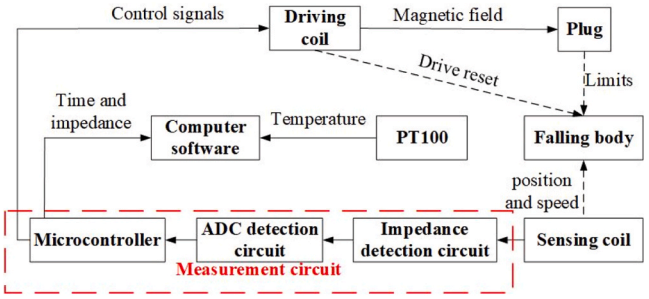

(a) System diagram

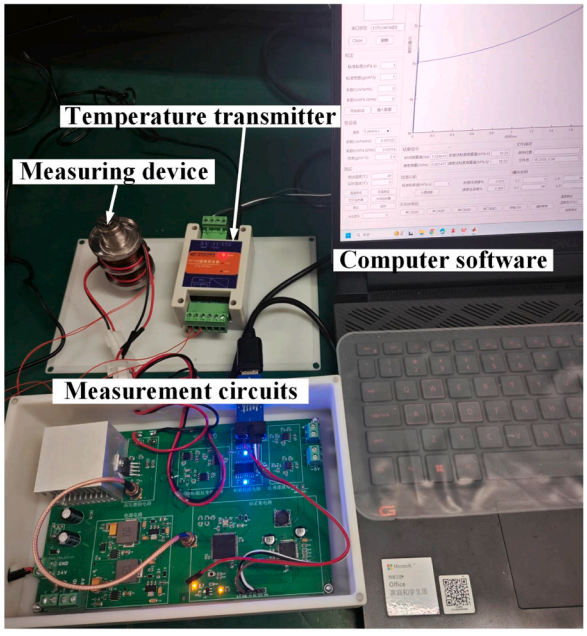

(b) Photo of the measurement system

Fig. 8. Measurement system.

4.2. Experimental results

The experimental samples included typical reference liquid squalane and diisodecyl phthalate as well as the national standard material GBW (E)130720 and the national standard material GBW(E)130615. The GBW(E)130720 was obtained from China Institute of Metrology. The GBW(E)130615 was obtained from China National Defense Science and Technology Industrial Applied Chemistry Level 1 Metrology Station. The squalane sample came from ShangHai EKEAR Bio&Tech Co. LTD, with a purity of 99 %. The diisodecyl phthalate sample was from Shanghai Macklin Biochemical Technology Co, Ltd, with a purity of 99 %. The viscosity values of different reference liquids at different temperatures are obtained from the literature [25,26,27] and national reference material identification certificates. (National reference material identification certificates are in the supplementary document)

(1) Verification of the viscosity measurement formula

The Z-t curves of FBs in the national standard material GBW(E) 130720 at different temperatures were tested. The radius of the FB r_1 is 3.93 mm. In the experiment, the timing starts when the driving coil is powered off, and the impedance value Z of the sensing coil is recorded at each moment. The results are shown in Fig. 9.

Fig. 9 shows that at 12530 ms and 18798 ms, the impedance value Z no longer changes, indicating that the FBs in the 298 K and 313 K standard liquids reach the lower limit. Before the FB reaches the lower limit, the coil impedance value Z is positively correlated with time t, and there is a linear region. A linear function is used to fit the data in the linear region, and two fitting straight lines are obtained: $Z = 0.00095t + 54.9623$ and $Z = 0.0014t + 55.0992$, as shown in Fig. 9. The fitted slopes k_{298} and k_{313} are the change rates of the coil impedance, and their values are 0.00095 and 0.0014, respectively, which are used to represent the stable speed v_s of the FB moving in two different liquids.

According to Eq. (2), in two liquids with little density change, the product of η and v_s should be a fixed value related to the size of the FB and the inner diameter of the stainless steel cylinder. The stable speed can be characterized by the change rate of the coil impedance, and the product of η and slope k should also be a fixed value C.

The viscosity values η_{298} and η_{313} obtained at 298 K and 313 K were 6.827 mPa·s and 4.417 mPa·s, respectively, according to the national calibration standard certificate. C is calculated as follows:

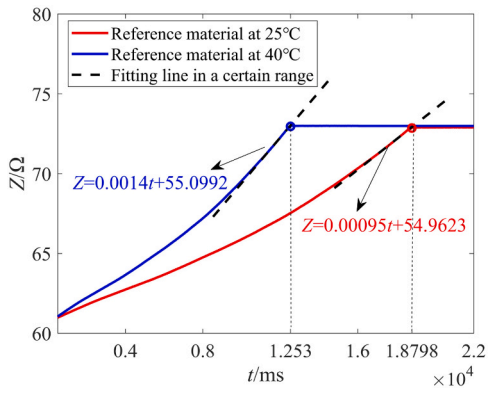

Fig. 9. Z-t test results.

$C_{298} = \eta_{298} * k_{298} = 6.827 * 0.00095 = 0.006485$

$C_{313} = \eta_{313} * k_{313} = 4.417 * 0.0014 = 0.006183$

The relative error of the calculated expected fixed value C is 4.6 %. The correctness of the measurement principle used is proven.

(2) Viscosity measurement results

①Squalane

The FB with r_1= 3.88 mm was used to measure the squalane liquid five times at temperatures of 298 K, 303 K, 308 K, 318 K, and 323 K. The measurement time was between 4 s~12 s. The measurement results were recorded as η_{m1}, η_{m2}, η_{m3}, η_{m4}, and η_{m5}. The average of five measurements $\overline{\eta}$ and the standard deviation σ are subsequently calculated. The reference viscosity values $\eta_r$of squalane at different temperatures were obtained from reference [23] and are recorded in Table 1. The error bar results of the viscosity test of squalane at different temperatures are shown in Fig. 10(a). Fig. 10(b) shows the relative error between each viscosity measurement value and the reference viscosity value at different temperatures. The percent deviation calculation formula is $(\eta_m - \eta_r)/\eta_r \times 100$.

Table 1 shows that the average value of the five measurements has a small difference from the reference value η_r obtained in reference [23]. The maximum absolute error occurs in the test result at a temperature of 318 K, which is 0.54 mPa·s. The standard deviation σ ranges from 0.18 to 0.74 mPa·s. Fig. 10(a) shows that the error bar is shorter when the temperature is higher and the viscosity is lower, which indicates that the experimental data of the viscosity test in squalane liquid are relatively stable and have small dispersion and high credibility. Fig. 10 (b) shows that the relative error between each measurement result and the reference viscosity is concentrated between −5 % and 5 %, with an average of 1.86 %. Within the 95 % confidence interval (k = 2), the expanded uncertainty of the squalane liquid viscosity measurement at different temperatures ranges from 0.78 mPa·s to 2.12 mPa·s, and the relative expanded uncertainty ranges from 6.13 % to 8.94 %, indicating that the designed experimental device and measurement method have high viscosity measurement accuracy.

②Diisodecyl phthalate

The FB with r_1= 3.79 mm was used to measure the diisodecyl phthalate liquid five times at temperatures of 298 K, 303 K, 308 K, 318 K, and 323 K. The measurement time was between 2 s~9 s. The measurement results were recorded as η_{m1}, η_{m2}, η_{m3}, η_{m4}, and η_{m5}. The average of five measurements $\overline{\eta}$ and the standard deviation σ are subsequently calculated. The reference viscosity values η_r of diisodecyl phthalate at different temperatures were obtained from references [24, 25] and are recorded in Table 2. The error bar results of the viscosity test of diisodecyl phthalate at different temperatures are shown in Fig. 11(a). Fig. 11(b) shows the relative error between each viscosity measurement value and the reference viscosity value at different temperatures.

Table 2 shows that the average value of the five measurements has a small difference from the reference value η_r obtained in references [24, 25]. The maximum absolute error occurs in the test result at 308 K, which is −1.93 mPa·s. The standard deviation σ ranges from 0.26 to 1.46 mPa·s. Fig. 11(a) shows that the error bar is shorter when the temperature is higher and the viscosity is lower, which shows that the experimental data of the viscosity test in diisodecyl phthalate liquid are relatively stable and have a small dispersion and high credibility. Fig. 11 (b) shows that the relative error between each measurement result and the reference viscosity is concentrated between −6 % and 3 %, with an average of −2.14 %. Within the 95 % confidence interval (k = 2), the expanded uncertainty of the diisodecyl phthalate liquid viscosity measurement at different temperatures ranges from 0.87 mPa·s to 4.27 mPa·s, and the relative expanded uncertainty ranges from 3.77 % to 5.07 %, indicating that the designed experimental device and measurement method have high viscosity measurement accuracy.

③GBW(E)130720

The FB with r_1= 3.93 mm was used to measure GBW(E)130720 five

Table 1
Viscosity test results of squalane at different temperatures T, unit: mPa·s.

T	298 K	303 K	308 K	313 K	318 K	323 K
η_{m1}	27.63	22.11	18.93	15.66	12.76	11.21
η_{m2}	27.25	22.01	18.75	15.27	13.20	11.10
η_{m3}	26.62	23.37	19.19	14.75	12.99	10.88
η_{m4}	28.49	22.72	17.57	15.86	13.20	11.26
η_{m5}	26.82	22.34	18.88	15.89	13.08	11.57
$\overline{\eta}$	27.36	22.51	18.67	15.49	13.05	11.20
σ	0.74	0.55	0.63	0.48	0.18	0.25
U (η)	2.12	1.66	1.67	1.29	0.80	0.78
U_{rel}/%	7.75	7.37	8.94	8.33	6.13	6.96
η_r[23]	27.87	22.7	18.15	15.2	12.5	10.7

Expanded uncertainties with a cover factor of k = 2 and 95 % confidence

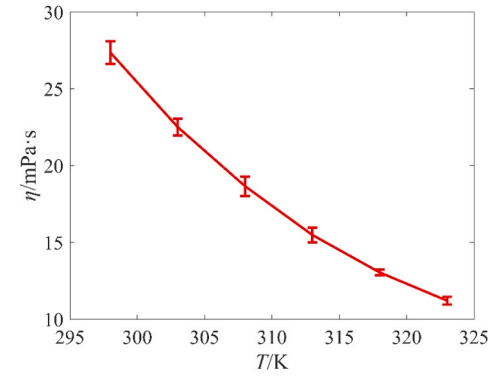

(a) Viscosity results

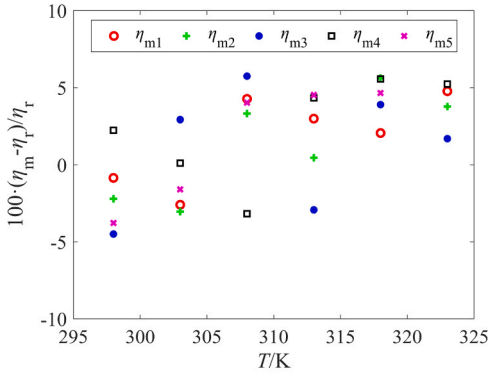

(b) Percent deviation

Fig. 10. Viscosity test results for squalane at different temperatures.

Table 2
Viscosity test results of diisodecyl phthalate at different temperatures T, unit: mPa·s.

T	298 K	303 K	308 K	313 K	318 K	323 K
η_{m1}	86.64	63.25	46.83	36.42	28.95	22.83
η_{m2}	89.14	62.99	47.27	36.82	28.75	23.15
η_{m3}	86.49	65.89	47.38	37.10	28.51	23.00
η_{m4}	89.75	64.63	47.77	38.34	28.75	22.96
η_{m5}	87.94	64.94	45.95	36.30	27.67	23.50
$\overline{\eta}$	87.99	64.34	47.04	37.00	28.53	23.09
σ	1.46	1.21	0.70	0.82	0.50	0.26
U (η)	4.27	3.26	2.11	1.99	1.36	0.87
U_{rel}/%	4.85	5.07	4.49	5.38	4.77	3.77
η_r[24,25]	88.5	65.0	48.98	38.01	29.43	23.56

Expanded uncertainties with a cover factor of k = 2 and 95 % confidence

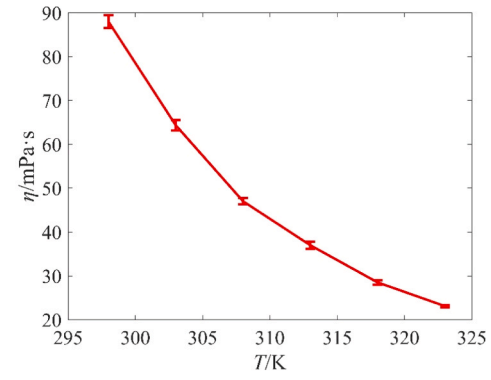

(a) Viscosity results

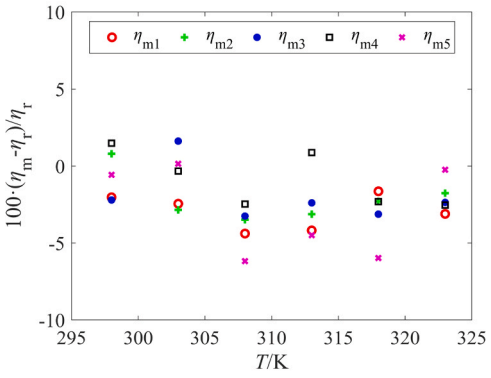

(b) Percent deviation

Fig. 11. Viscosity test results of diisodecyl phthalate at different temperatures.

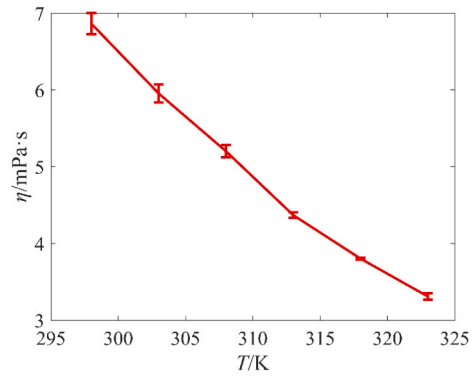

(a) Viscosity results

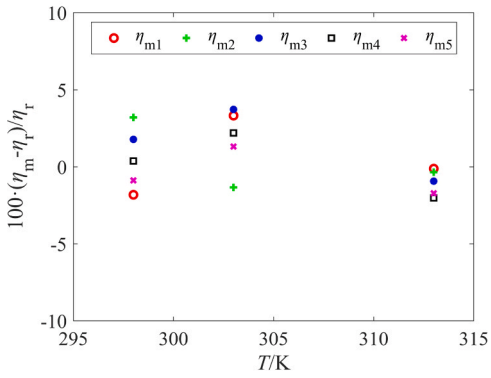

(b) Percent deviation

Fig. 12. Viscosity test results of GBW(E)130720 at different temperatures.

times at temperatures of 298 K, 303 K, 308 K, 318 K, and 323 K. The measurement time ranged from 9 to 19 s. The measurement results are recorded as η_{m1}, η_{m2}, η_{m3}, η_{m4}, and η_{m5}. The average of five measurements $\overline{\eta}$ is then calculated, and the standard deviation σ is calculated. The reference viscosity values η_r of GBW(E)130720 at different temperatures were obtained from the standard material identification certificate and are recorded in Table 3. The error bar results of the viscosity test of diisodecyl phthalate at different temperatures are shown in Fig. 12(a). Fig. 12(b) shows the relative error between each viscosity measurement value and the reference viscosity value at different temperatures.

Table 3 shows that the average value of the five measurements has a small difference from the reference value η_r obtained from the standard material identification certificate. The maximum absolute error occurs in the test result at 303 K, which is 0.1 mPa·s, and the standard deviation

Table 3
Viscosity test results of GBW(E)130720 at different temperatures *T*, unit: mPa·s.

T	298 K	303 K	308 K	313 K	318 K	323 K
η_{m1}	6.70	6.04	5.14	4.41	3.82	3.24
η_{m2}	7.05	5.77	5.31	4.40	3.80	3.30
η_{m3}	6.95	6.07	5.26	4.38	3.82	3.33
η_{m4}	6.85	5.98	5.20	4.33	3.80	3.34
η_{m5}	6.77	5.93	5.11	4.34	3.78	3.35
$\overline{\eta}$	6.86	5.96	5.20	4.37	3.80	3.31
σ	0.14	0.12	0.08	0.04	0.01	0.04
U (η)	0.48	0.41	/	0.26	/	/
U_{rel}/%	7	6.88	/	5.95	/	/
η_r [#]	6.827	5.848	/	4.417	/	/

#: Obtained from calibration certificates issued by the National Applied Chemistry Level 1 Metrology Station.
Expanded uncertainties with a cover factor of $k = 2$ and 95 % confidence

σ ranges from 0.01 to 0.14 mPa·s. Fig. 12(a) shows that the error bar is shorter when the temperature is higher and the viscosity is lower, which shows that the viscosity test experimental data in the GBW(E)130720 liquid are relatively stable. Fig. 12(b) shows that the relative error between each measurement result and the reference viscosity is concentrated between −4 % and 5 %, with an average of 0.45 %. Within the 95 % confidence interval ($k = 2$), the expanded uncertainty of the GBW(E)130720 liquid viscosity measurement at different temperatures ranges from 0.26 mPa·s to 0.48 mPa·s, and the relative expanded uncertainty ranges from 5.95 % to 7 %, indicating that the designed experimental device and measurement method have high viscosity measurement accuracy.

④GBW(E)130615

The FB with r_1= 3.88 mm was used to measure the GBW(E)130615 liquid five times at temperatures of 298 K, 303 K, 308 K, 318 K, and 323 K. The measurement time was between 4 s∼13 s. The measurement results were recorded as η_{m1}, η_{m2}, η_{m3}, η_{m4}, and η_{m5}. The average of five measurements $\overline{\eta}$ and the standard deviation σ are subsequently calculated. The reference viscosity values $\eta_r$of GBW(E)130615 at different temperatures were obtained from the standard material identification certificate and are recorded in Table 3. The error bar results of the viscosity test of squalane at different temperatures are shown in Fig. 13(a). Fig. 13(b) shows the relative error between each viscosity measurement value and the reference viscosity value at different temperatures.

Table 4 shows that the average value of the five measurements has a small difference from the reference value η_r obtained from the standard material identification certificate. The maximum absolute error occurs in the test result at a temperature of 298 K, which is −1.15 mPa·s, and the standard deviation σ ranges from 0.15 to 0.23 mPa·s. Fig. 13(a) shows that the error bar is shorter when the temperature is higher and the viscosity is lower, which shows that the viscosity test experimental data in the GBW(E)130615 liquid are relatively stable. Fig. 13(b) shows

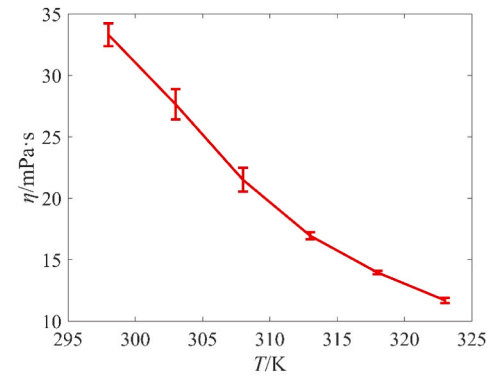

(a) Viscosity results

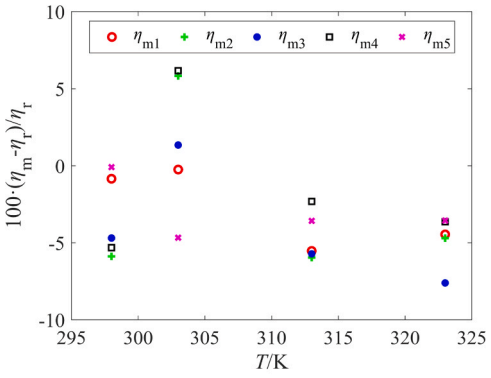

(b) Percent deviation

Fig. 13. Viscosity test results of GBW(E)130615 at different temperatures.

Table 4
Viscosity test results of GBW(E)130615 at different temperatures T, unit: mPa·s.

T	298 K	303 K	308 K	313 K	318 K	323 K
η_{m1}	34.18	27.12	20.86	16.79	14.02	11.74
η_{m2}	32.44	28.78	21.93	16.71	14.19	11.71
η_{m3}	32.85	27.56	21.24	16.76	13.94	11.36
η_{m4}	32.64	28.87	20.52	17.36	13.83	11.84
η_{m5}	34.44	25.92	22.97	17.14	13.84	11.85
$\overline{\eta}$	33.31	27.65	21.51	16.95	13.96	11.70
σ	0.93	1.23	0.97	0.28	0.15	0.20
U (η)	2.63	2.93	/	1.09	/	0.74
U_{rel}/%	7.9	10.6	/	6.43	/	6.32
η_r [#]	34.47	27.19	/	17.77	/	12.29

#: Obtained from calibration certificates issued by the National Applied Chemistry Level 1 Metrology Station.
Expanded uncertainties with a cover factor of $k = 2$ and 95 % confidence

that the relative error between each measurement result and the reference viscosity is concentrated between −7 % and 6 %, with an average of −2.76 %. Within the 95 % confidence interval ($k = 2$), the expanded uncertainty of the GBW(E)130615 liquid viscosity measurement at different temperatures ranges from 0.74 mPa·s to 2.93 mPa·s, and the relative expanded uncertainty ranges from 6.32 % to 10.6 %, indicating that the designed experimental device and measurement method have high viscosity measurement accuracy.

⑤ Temperature control problem

It should be noted that the current temperature control method in the experiment will lead to the generation of temperature gradients within the device, which is also a reason for the measurement error in the viscosity test results. We will improve the device in the future by setting a water bath sandwich between the actuation and heating coil and the closed cavity. The temperature of the device wall and the liquid in the device is precisely controlled by means of a water bath to avoid the generation of temperature gradients between the temperature monitoring point and the liquid.

5. Summary and outlook

5.1. Summary

(1) In this paper, we propose a viscosity measurement device and method for liquids in a CCC, which uses the sensitivity change rate of the detection coil to characterize the steady velocity of the FB. The device is characterized by a simple structure, small size, low sample volume requirements and fast detection speed.
(2) In this device, the drop distance is only 11 mm. For squalane, diisodecyl phthalate, the standard material GBW(E)130720, and the standard material GBW(E)130615, with a temperature range of 298–323 K, the viscosity range is 4.417–88.44 mPa·s. Only 1 mL of sample is needed to measure the viscosity, and the falling time of the FB is 2–19 s, which is faster than that of the traditional FB method.
(3) The viscosity of the above four different liquids was measured through the designed viscosity measurement device and measurement method. The results have high accuracy and high repeatability. The relative error is concentrated within 5 %, and the standard deviation is between 0.01 mPa·s and 1.46 mPa·s. Within the 95 % confidence interval ($k = 2$), the expanded uncertainty of the four liquid viscosity measurements at different temperatures ranges from 0.26 mPa·s to 4.27 mPa·s, and the relative expanded uncertainty ranges from 3.77 % to 10.6 %.

5.1.1. Outlook

We designed inlet and outlet ports for the proposed liquid viscosity measurement device to conveniently replace the liquid in the CCC under high-temperature and high-pressure conditions. The aforementioned tests were conducted with this structure, which can be directly connected to high-temperature and high-pressure generating devices for testing. In the next step, we will design a high-temperature and high-pressure liquid generator and design a water bath device for precise temperature control.

CRediT authorship contribution statement

Ma Jinyu: Writing – original draft, Visualization, Software, Methodology, Formal analysis, Data curation, Conceptualization. **Li Jian:** Supervision, Software, Resources. **Huang Xinjing:** Methodology, Investigation, Funding acquisition, Conceptualization. **Bian Xu:** Visualization, Validation, Supervision. **Zhang Hongbin:** Writing – review & editing, Investigation, Data curation. **Zhang Kun:** Supervision, Software, Resources.

Declaration of Competing Interest

The authors have declared no conflict of interest.

Acknowledgments

This work was supported in part by the National Natural Science Foundations of China (Nos 62473279 and 62073233), and Guangxi Key Laboratory of Automatic Detecting Technology and Instruments Foundation (No. YQ24203).

Appendix A. Supporting information

Supplementary data associated with this article can be found in the online version at doi:10.1016/j.sna.2025.116401.

Data availability

Data will be made available on request.

References

[1] H.L. Wang, Z. Li, J.W. Zhao, Discussion of viscosity measurement of liquids, Phys. Exp. Coll. 02 (1994) 33–35.
[2] B.H. Shi, S. Chai, L.Y. Wang, X. Lv, H.S. Liu, H.H. Wu, W. Wang, D. Yu, J. Gong, Viscosity investigation of natural gas hydrate slurries with anti-agglomerants additives, Fuel 185 (2016) 323–338.
[3] S. Gautam, C. Guria, L. Gope, Prediction of high-pressure/high-temperature rheological properties of drilling fluids from the viscosity data measured on a coaxial cylinder viscometer, SPE J. 26 (05) (2021) 2527–2548.
[4] Y.F. Guo, Research on the current situation and high-quality development path of coal-to-liquid: research on the high-quality development of coal direct liquefaction technology, Inn. Mong. Petrochem. Ind. 47 (09) (2021) 4–8.
[5] E. Jenab, F. Temelli, Viscosity measurement and modeling of canola oil and its blend with canola stearin in equilibrium with high pressure carbon dioxide, J. Supercrit. Fluids 58 (1) (2011) 7–14.
[6] M. Hosoda, Y. Yamakawa, K. Sakai, Electromagnetically spinning viscometer designed for measurement of low viscosity in low shear rate region, Jpn. J. Appl. Phys. 63 (4) (2024) 04SP16.
[7] M.E. Kandil, K.N. Marsh, A.R.H. Goodwin, Vibrating Wire Viscometer with Wire Diameters of (0.05 and 0.15) mm: Results for Methylbenzene and Two Fluids with Nominal Viscosities at T=298 K and p=0.01 MPa of (14 and 232) mPa·s at Temperatures between (298 and 373) K and Pressures below 40 MPa, J. Chem. Eng. Data 50 (2) (2005) 647–655.
[8] J.B. Zhang, X.Y. Meng, G.S. Qiu, J.T. Wu, Development of vibrating-wire viscometer for liquid at high pressure, J. Xi'an Jiaotong Univ. 46 (11) (2012) 30–34.
[9] P.W. Bridgman, The viscosity of liquids under pressure, Proc. Natl. Acad. Sci. U. S. A. 11 (10) (1925) 603–606.
[10] P.W. Bridgman, The effect of pressure on the viscosity of forty-three pure liquids, Proc. Am. Acad. Arts Sci. 61 (3) (1926) 57–99.
[11] K.R. Harris, A falling body high-pressure viscometer, Int. J. Thermophys. 44 (12) (2023) 184.
[12] S. Bair, A routine high-pressure viscometer for accurate measurements to 1 GPa, Tribol. Trans. 47 (3) (2004) 356–360.
[13] Y. Tanaka, Y. Matsuda, H. Fujiwara, H. Kubota, T. Makita, Viscosity of (water+ alcohol) mixtures under high pressure, Int. J. Thermophys. 8 (1987) 147–163.
[14] Y. Tanaka, T. Yamamoto, Y. Satomi, H. Kubota, T. Makita, Specific volume and viscosity of ethanol-water mixtures under high pressure, Rev. Phys. Chem. Jpn. 47 (1) (1977) 12–24.
[15] R.K.Y. Chan, D.A. Jackson, An automated falling-cylinder high pressure laser-Doppler viscometer, J. Sci. Instrum. 18 (6) (1985) 510.
[16] A. Dandridge, D.A. Jackson, Measurements of viscosity under pressure: a new method, J. Phys. D: Appl. Phys. 14 (5) (1981) 829.
[17] X.J. Wang, S.S. Zhu, X.P. Wang, F.X. Yang, Experimental system for high-pressure viscosity measurement based on the falling-body method, J. Eng. Thermophys. 41 (04) (2020) 788–791.
[18] C.J. Schaschke, S. Allio, E. Holmberg, Viscosity measurement of vegetable oil at high pressure, Food Bioprod. Process. 84 (3) (2006) 173–178.
[19] C.J. Schaschke, S. Abid, I. Fletcher, M.J. Heslop, Evaluation of a falling sinker-type viscometer at high pressure using edible oil, J. Food Eng. 87 (1) (2008) 51–58.
[20] J.B. Irving, A.J. Barlow, An automatic high pressure viscometer, J. Sci. Instrum. 4 (3) (1971) 232.
[21] D.I. Sagdeev, M.G. Fomina, G.Kh Mukhamedzyanov, I.M. Abdulagatov, Experimental study of the density and viscosity of polyethylene glycols and their mixtures at temperatures from 293 K to 473 K and at atmospheric pressure, J. Chem. Thermodyn. 43 (12) (2011) 1824–1843.
[22] D.I. Sagdeev, M.G. Fomina, G.Kh Mukhamedzyanov, I.M. Abdulagatov, Experimental study of the density and viscosity of polyethylene glycols and their mixtures at temperatures from 293 K to 465 K and at high pressures up to 245 MPa, Fluid Phase Equilib. 315 (2012) 64–76.
[23] M.J. Comuñas, X. Paredes, F.M. Gaciño, J. Fernández, J.P. Bazile, C. Boned, J. L. Daridon, G. Galliero, J. Pauly, K.R. Harris, M.J. Assael, S.K. Mylona, Reference correlation of the viscosity of squalane from 273 to 373 K at 0.1 MPa, J. Phys. Chem. Ref. Data 42 (3) (2013).
[24] A.P. Fröba, A. Leipertz, Viscosity of diisodecyl phthalate by surface light scattering (SLS), J. Chem. Eng. Data 52 (5) (2007) 1803–1810.
[25] F.J. Caetano, J.M. Fareleira, A.P. Fröba, K.R. Harris, A. Leipertz, C.M. Oliveira, J.P. Martin Trusler, W.A. Wakeham, An industrial reference fluid for moderately high viscosity, J. Chem. Eng. Data (9) (2008) 2003–2011.

Xinjing Huang received the B. E. and Ph. D. degrees in instrument science and technology from Tianjin University, Tianjin, China, in 2010 and 2016, respectively. He is currently an Associate Professor with the School of Precision Instrument and Opto-Electronics Engineering, Tianjin University, where he also works with the State Key Laboratory of Precision Measurement Technology and Instruments. His research topics mainly cover acoustic and/or electromagnetic sensing and measurement technologies.

Hongbin Zhang received the B. Sc. degree in measurement and control technology and instrument from Hebei University of Technology, Tianjin, China, in 2022. He is currently pursuing the M. Sc. degree in Tianjin University, under the guidance of Associate Professor Xinjing Huang. His research interests include pipeline stress measurement, signal feature extraction, and the application of magnetic sensors.

Bian Xu received the Ph.D. degree from Tianjin University, in 2016. He is currently a post doctor with the Instrument Science and Technology Department in Tianjin University and a lecturer in Tianjin Renai College. His research interests include pressure vessel leakage detection, viscosity measurement and structural health monitoring.

Kun Zhang received her master's degree in analytical chemistry from Jilin University (Changchun) in 2008. Currently working at Shandong Non-Metal Materials Research Institute. Her research interests mainly involve chemical measurement and viscosity and density detection technology.

Jian Li received his B.E., M.E., and Ph.D. degrees in Instrument Science and Technology from Tianjin University, Tianjin, China, in 1994, 1997, and 2000, respectively. He is currently a full professor in the School of Precision Instrument and Opto-Electronics Engineering at Tianjin University. He also works at State Key Laboratory of Precision Measurement Technology and Instrument, Tianjin University. His research topics mainly cover test signal processing, weak signal detection, and target detection technology and instruments.

Jinyu Ma received her B. E. and M. E. degrees both in Instrument Science and Technology from Shandong University of Science and Technology, Qingdao, China, in 2010 and 2012, respectively. She received her Ph. D. degree in Instrument Science and Technology from Tianjin University, Tianjin, China, in 2016. In 2016, she joined the Sensor and Electronic Testing Laboratory of Tianjin University as a lecturer and engineer. She also works at State Key Laboratory of Precision Measurement Technology and Instrument, Tianjin University. Her research topics mainly cover electric sensing and measurement, precision measuring circuit, measurement and control based on embedded system.